J. appl. Chem. Biotechnol. 1975, **25**, 707–720

Oxygen Transfer Coefficients by the Dynamic Method

Irving J. Dunn[a] and Arthur Einsele[b]

[a]*Technisch-chemisches Laboratorium,* [b]*Institut für Mikrobiologie,*
Swiss Federal Institute of Technology, Zürich, Switzerland

(*Paper received 11 December 1974, amended paper accepted 27 January 1975*)

Models useful in the dynamic method for K_La measurements are developed and compared. Particular attention is given to the gas phase dynamics and the oxygen electrode response time. Comparisons and error calculations are based on computer simulations. Correction factors are presented for a range of dimensionless parameters. In general, the errors resulting from neglecting the gas phase dynamics and the electrode response can be expected to be large.

1. Introduction

Aerobic fermentations are dependent on the supply of oxygen to the liquid phase. Indeed, industrial fermentations are often limited in their productivity by the oxygen transfer rate. One of the primary parameters on which to judge fermenter operating performance and to base fermenter scale-up is the oxygen transfer rate. This can be expressed in terms of a mass transfer coefficient K_La, if the driving force, $C_L^* - C_L$, can be evaluated. This information can be provided if the partial pressure of oxygen and its concentration in the liquid phase can be measured. Thus, for example a steady state oxygen balance on the fermenter gas stream yields the oxygen transfer rate (OTR), and the simultaneous measurement of the dissolved oxygen, along with assumptions regarding the flow patterns of gas in the fermenter (e.g. well-mixed or plug flow), allows the calculation of K_La during fermentation.

For the purpose of comparing fermenters on an oxygen transfer efficiency basis, it is often desirable to evaluate the mass transfer coefficient without the presence of biological growth. This can be accomplished using several methods:

1. The sulphite method[1] is a steady state method involving the chemical oxidation of sodium sulphite to sodium sulphate. The extent of reaction is normally followed by titration, but gas analysis can also be employed to determine the oxygen transfer rate or as a check on the titration. This method does not completely characterise a fermenter because of the enhancement effects[2] that the chemical reaction has on the oxygen transfer rate.

2. A continuous steady state method can be devised by providing the fermenter

vessel with a steady supply of deoxygenated liquid. The required analyses are liquid and gas flow rates, dissolved oxygen, and gaseous oxygen. Use of this method has been made for oxygen transfer in fermenters,[2] and it has been employed for various gas–liquid systems.[3]

3. The dynamic oxygen electrode method involves measuring the response of dissolved oxygen in a batch liquid to changing gas conditions.[4] It requires a rapidly responding, continuously recording instrument. Since the development of the sterilisable-membrane oxygen electrode, this method has been widely used in fermentation.[2,5–8]

Dynamic methods require the use of models to describe the time varying process in terms of the measured variables, thus allowing calculation of the desired parameters. The dynamic K_La method has been the subject of numerous papers giving particular attention to complex electrode response models.[2,7,8] It appears that little attention has been paid to the description of the dispersed gas phase. Simplified models have often been employed because the simpler parameter estimation procedures used in calculating K_La from the response data have required an analytically integratable model.

The objective of the present paper is to draw attention to the errors which can accrue from simplified models. The possible model equations are developed and compared qualitatively on the basis of the governing dimensionless parameters. Numerical simulations provide an exact comparison between models for particular parameter combinations. Particular emphasis is given to estimating the errors which can arise when the dispersed gas phase dynamics and the electrode response time are neglected. The results presented enable the investigator to choose a model for his own system which will give error-free K_La values or to correct values obtained from invalid models.

2. Theory

The approach taken here will be to describe the fermenter in terms of well-mixed dispersed gas and liquid phases. For large-scale fermenters there is considerable reason to believe that this assumption is not generally valid, although little data is available in the literature on this subject. Small fermenters with high stirring energy inputs can be generally expected to possess well-mixed dispersed gas and liquid phases.[9] The gas composition in the head space above the liquid will not, except for very high stirring rates, be the same as that which is dispersed in the liquid. In what follows the term "gas phase" refers to the gas which is dispersed. For actual fermenter performance the question of whether the gas phase should be represented by a well-mixed or plug model may not be important. This is because the inlet and outlet gas streams have very nearly the same oxygen concentration in many practical fermentation processes. On the other hand, an exact description of the gas phase is very important for the proper evaluation of the dynamic K_La method, because of the nature of the experiment, which begins with the fermenter being full of the nitrogen used for degassing.

2.1. Well-mixed gas phase models

Well-mixed gas phase:

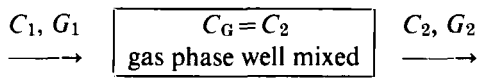

Homogeneity will prevail throughout the gas phase. Thus, the exit gas will have the same concentration as the system concentration, $C_G = C_2$.

Formulating the general oxygen mass balance:

$$\begin{pmatrix}\text{accumulation rate}\\ \text{of } O_2 \text{ within the}\\ \text{gas phase}\end{pmatrix} = \begin{pmatrix}\text{rate of flow}\\ \text{of } O_2 \text{ into}\\ \text{the gas phase}\end{pmatrix} - \begin{pmatrix}\text{rate of flow}\\ \text{of } O_2 \text{ out of}\\ \text{the gas phase}\end{pmatrix} - \begin{pmatrix}\text{rate of transfer}\\ \text{of } O_2 \text{ out of}\\ \text{the gas phase}\end{pmatrix}$$

In mathematical terms:

$$\frac{d(V_G C_2)}{dt} = G_1 C_1 - G_2 C_2 - K_L a\,(C_L^* - C_L).\,V_L$$

A total mass balance shows that if the gas phase volume remains constant and the densities of entering and exit gas are the same, then $G_1 = G_2$.

Using these assumptions, the oxygen gas balance becomes

$$\frac{dC_2}{dt} = \frac{C_1 - C_2}{(V_G/G)} - K_L a\,(C_L^* - C_L)\,\frac{V_L}{V_G} \qquad \textit{Model GI}$$

Model GI assumptions: (a) well-mixed gas phase; (b) V_G = constant; (c) $G_1 = G_2$.

When the accumulation rate and the transfer rate are small compared with the flow terms, the simplest model results in $C_1 = C_2$. This is model GII.

Model GII assumptions: (*a*) well-mixed gas phase; (b) V_G = constant; (c) $G_1 = G_2$; (d) accumulation and transfer terms negligible.

When the incoming stream is air, model GII says that at all times air will be in contact with the liquid phase. The utility of model GII lies in its simplicity. It results, as will be shown, in a simple mathematical model for both phases. Consideration of all the terms in model GI leads one to the conclusion that for certain values of the governing parameters, V_G, V_L, $K_L a$, G and C^*, the other terms may be important. If only the transfer term is neglected model GI becomes:

$$\frac{dC_2}{dt} = \frac{C_1 - C_2}{\tau_G} \qquad \textit{Model GIII}$$

where τ_G is the gas phase mean residence time, V_G/G.

Model GIII assumptions: (a) well-mixed gas phase; (b) $G_1 = G_2$; (c) transfer terms small.

This equation is of the form known in dynamics as a first order lag. It can be easily combined with the liquid phase model to obtain an analytical solution because it is not coupled to the liquid phase through C_L.

Neglecting only the accumulation, $dC_2\,dt$, in model GI results in a steady state oxygen balance,

$$O=\frac{C_1-C_2}{\tau_G}-K_La\,(C_L^*-C_L)\frac{V_L}{V_G} \qquad \textit{Model GIV}$$

The advantage in this model is that it is an algebraic equation and can be handled more easily than a differential equation model.[2]

2.2. Well-mixed liquid phase model

The general O_2 mass balance formulation for the liquid phase is:

$$\begin{pmatrix}\text{accumulation rate}\\ \text{of } O_2 \text{ in the}\\ \text{liquid}\end{pmatrix}=\begin{pmatrix}\text{rate of transfer}\\ \text{of } O_2 \text{ into the}\\ \text{liquid}\end{pmatrix}$$

Normally, mass transfer experiments are conducted with an organism-free batch liquid. For this reason, flow and cell oxygen uptake terms do not appear in the equation. In mathematical symbols:

$$\frac{d\,(V_LC_L)}{dt}=K_La\,(C_L^*-C_L).\,V_L$$

For constant volume:

$$\frac{dC_L}{dt}=K_La\,(C_L^*-C_L) \qquad \textit{Liquid model}$$

Liquid model assumptions: (a) well-mixed batch liquid; (b) V_L=constant; (c) no uptake by cells.

2.3. Combined models for oxygen transfer coefficient determination

The mathematical description used to calculate the oxygen transfer rate coefficient in the fermenter must involve a combination of the appropriate gas and liquid phase oxygen balances. For well-mixed systems (gas and liquid), involving continuous gas flow and batch liquid, the possible models are as follows:

Model I = models GI and liquid model
Model II = models GII and liquid model
Model III = models GIII and liquid model
Model IV = models GIV and liquid model.

In each of the above models the saturation concentration of O_2 in the liquid, C_L^*, appears. To evaluate this, each model requires the equilibrium relation between C_2 and C_L. For gases of low solubility this is supplied by Henry's law:

$$P_i=H_{i,j}\,C_{L\,i,j}^*$$

where i refers to the component and j refers to the particular liquid involved. Assuming an ideal gas phase converts the partial pressure relation into an equilibrium relation-

ship between the gas phase oxygen concentration and the liquid phase oxygen concentration,

$$C_2 = \frac{H}{RT} C_L^*$$

In order to ascertain the validity of the assumptions made in formulating models I, II, III and IV, it is necessary to consider the nature of the dynamic $K_L a$ experiment and the magnitudes of the governing parameters, and to compare the solutions of the models for different parameter values.

The experiment is started at a very low dissolved oxygen concentration. This is achieved by degassing with nitrogen. Initially C_L and C_2 are equal to zero because the liquid has been degassed and the gas phase contains only nitrogen.

The gas stream can be switched from nitrogen to air without disrupting the gas hold up appreciably if the flow rates are the same. As air enters the system it mixes with the nitrogen bubbles. The oxygen concentration C_2 will rise as the air washes out the remaining nitrogen. During this period oxygen is transferred to the liquid phase. The liquid phase concentration is measured with an oxygen electrode.

The ratio of washout rate to transfer rate will be determined by how fast the nitrogen is removed by the entering air stream. These relative rates can be qualitatively examined by formulating the equations in dimensionless form and comparing the magnitude of the dimensionless parameters which appear in the resulting equations. Defining the dimensionless concentrations with ranges between zero and unity,

$$\bar{C}_2 = C_2/C_1$$

$$\bar{C}_L = \frac{C_L}{(C_1 RT/H)}$$

The dimensionless time is related to the mass transfer coefficient. Thus,

$$\bar{t} = K_L a \,.\, t$$

With these dimensionless variables model I becomes:

Gas phase:
$$\frac{d\bar{C}_2}{d\bar{t}} = \frac{1-\bar{C}_2}{(K_L a \tau_G)} - \left[\frac{V_L}{V_G}\right] \cdot \left[\frac{RT}{H}\right] (\bar{C}_2 - \bar{C}_L)$$

Liquid phase:
$$\frac{d\bar{C}_L}{d\bar{t}} = (\bar{C}_2 - \bar{C}_L)$$

Initial conditions: $\bar{t}=0$; $\bar{C}_L=0$; $\bar{C}_2=0$.

The dimensionless parameters which govern the solution to model I are the transfer-flow group, $K_L a \tau_G$, and the liquid–gas volume ratio, V_L/V_G. Distinction should be made between this volume ratio and the hold up, $V_G/(V_L+V_G)$. The group RT/H is a constant for the oxygen–water system at constant temperature. Model I is the general model and models II, III and IV represent simplifications and are obtained by neglecting terms in the general model.

In evaluating the conditions for which certain terms can be neglected, it is useful to consider the physical significance of the dimensionless parameters:

$$K_L a\,\tau_G = \frac{\text{O}_2 \text{ transfer rate}}{\text{rate of O}_2 \text{ supply by flow}}$$

$$\frac{V_L}{V_G}\frac{RT}{H} = \frac{\text{moles O}_2 \text{ in liquid at equilibrium}}{\text{moles O}_2 \text{ in gas at equilibrium}}$$

To estimate the expected magnitudes of the terms in model I it is sufficient to consider the values of the dimensionless parameters. Clearly, when $K_L a\tau_G$ is small (O_2 supply by flow $\gg O_2$ transfer rate), the time derivative $d\bar{C}_2/d\bar{t}$ may be large, providing that V_L/V_G is not too large. In this case the term containing V_L/V_G can be completely neglected, since $RT/H \approx 0.03$. Thus,

$$\frac{d\bar{C}_2}{d\bar{t}} = \frac{1-\bar{C}_2}{\begin{pmatrix}\text{number}\\ \ll 1.0\end{pmatrix}} - \underbrace{\begin{pmatrix}\text{number}\\ > 1.0\end{pmatrix}\cdot\left(\frac{RT}{H}\right)(\bar{C}_2 - C_L)}_{\text{neglect this term}}$$

The resulting approximation becomes equivalent to model II because if C_2 increases rapidly it will very shortly be equal to the concentration in the incoming air stream. The dimensionless time constant for this process is equal to $K_L a\tau_G$. It can be shown that when $\bar{t} = K_L a\tau_G$, $\bar{C}_2$ has risen to 63.2% of $\bar{C}_1$. On a real time basis, when $t = 4\tau_G$, the process is 99% complete. By such considerations of the relative order of magnitude of the dimensionless parameters, it is possible to predict under what conditions models II, III and IV will be valid, as shown in Table 1.

Table 1. Conditions for validity

Model I	$K_L a\tau_G$ (general case)	$\approx \frac{V_L}{V_G}\cdot\frac{RT}{H} \approx 1.0$
Model II	$K_L a\tau_G$	$\ll 1.0$
	$\frac{V_L}{V_G}\cdot\frac{RT}{H}$	$\ll 1.0$
Model III	$K_L a\tau_G$	< 1.0
	$\frac{V_L}{V_G}\cdot\frac{RT}{H}$	$\ll 1.0$
Model IV	$K_L a\tau_G$	< 1.0
	$\frac{V_L}{V_G}\cdot\frac{RT}{H}$	> 1.0

Although it is possible to identify the above limiting situations, it is not possible by this method to determine the approximate error which will arise in the calculated $K_L a$ value when an invalid model is assumed. This determination requires a numerical solution of the corresponding models for particular values of $K_L a\tau_G$ and V_L/V_G and a comparison with the general model.

2.4. Comparison of models and associated errors

Many investigators reporting K_La measurements have utilised model II to analyse their dynamic measurements of C_L and to calculate K_La values. Model II is given by the following dimensionless equation:

$$\frac{d\bar{C}_L}{d\bar{t}} = (\bar{C}_2 - \bar{C}_L)$$

and initial conditions:

$$\bar{t} = 0,\ \bar{C}_L = 0$$

$$\bar{C}_2 = 1.0 = \text{constant at all } \bar{t}.$$

The integration gives

$$-\ln(1 - \bar{C}_L) = \bar{t} + K$$

where $K = -\ln(1) = 0$.

Thus the solution is:

$$\ln\left(\frac{1}{1 - \bar{C}_L}\right) = \bar{t}$$

In dimensional form:

$$\ln\left(\frac{1}{1 - (\bar{C}_L)/C^*_{L\text{air}}}\right) = K_La.t$$

where $C^*_{L\text{air}}$ is the liquid phase oxygen concentration in equilibrium with air.

A plot of

$$\ln\left(\frac{C_{L\text{air}}^*}{C^*_{L\text{air}} - C_L}\right) \text{ vs } t$$

gives a slope of K_La.[4]

The measurement of C_L against time involves the question of the electrode response time which will be assumed to be very small. The errors resulting from larger response times will be treated later.

If model II were assumed to be valid, K_La would be determined by plotting the data as indicated and obtaining the slope. The value thus obtained would be the value of K_La calculated by applying model II or K_La_{II}. In what follows subscripts on K_La refer to the entire K_La quantity.

The value of K_La_{II} can be compared to the value derived from the general model, K_La_I, to provide a measure of the error which results from applying model II. The real physical situation is assumed here to be exactly described by model I.

Similarly, the results obtained by applying models III and IV can be compared to those from model I for particular values of the parameters. Thus, numerical solutions of the models have been computed and a comparison drawn between the "apparent" and "true" values of K_La as a fraction of the parameters $K_La\tau_G$ and V_L/V_G.

2.5. Electrode dynamics

In the foregoing analysis the possibility of measuring C_L without considering the dynamic characteristics of the electrode has been assumed. Generally, sterilisable

electrodes, which are commercially available, exhibit rather long response times. This is because of the diffusion process which must take place through a membrane before oxygen reaches the electrode.

Although more complex models have been proposed and used to describe the electrode dynamics, experience in our laboratories and elsewhere[5] has shown that a first order equation of the form:

$$\frac{dP_E}{dt} = \frac{C_L . H - P_E}{\tau_E} \qquad \textit{Electrode model}$$

is adequate.

The term P_E represents the oxygen partial pressure at the electrode and τ_E is the time constant of the electrode. The time constant, τ_E, can be easily measured by subjecting the electrode to a sudden known step change in C_L and measuring the time for the response to be 63.2% complete. Care must be taken to establish that the time constant is independent of the turbulent conditions in the liquid phase. Recent experiments show that this can be generally assumed only for very thick membranes and high stirring rates. An investigator who has no appreciation for the importance of electrode dynamics may believe that he is measuring the true value of C_L. Assuming, as before, that model II is valid, his logarithmic plot will yield an apparent value of K_La which is influenced by two factors, the gas dynamics and the electrode dynamics. This apparent value is designated as K_La_{IIE}.

3. Results and discussions of computer simulations

The fractional deviation of K_La_{II} from the true value, K_La_I, is expressed as the ratio, $(K_La_I - K_La_{II})/K_La_I$. The fractional deviation from the true value will vary between zero ($K_La_I = K_La_{II}$) and unity ($K_La_{II} = 0$). Its value will be a function of the system parameters $[K_La\tau_G]$ and $[V_L/V_G]$. In what follows K_La without subscript indicates the true value.

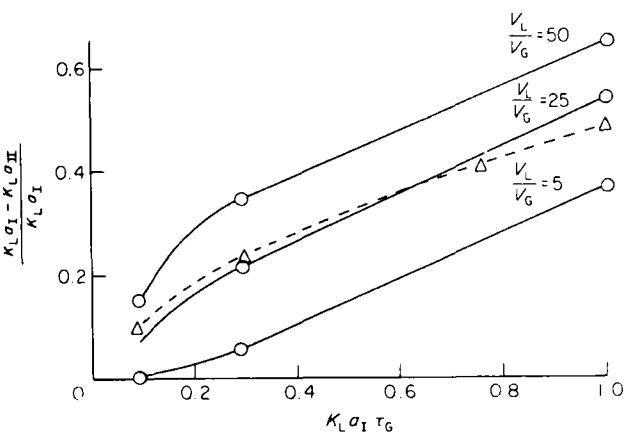

Figure 1. Fractional error in K_La accrued from model II as a function of system parameters. - - - -, Approximation; ——, simulation.

Figure 1 shows plots of the fractional $K_L a$ deviation *vs* $[K_L a \tau_G]$ for three $[V_L/V_G]$ values as obtained from computer simulations. Here it is clearly shown that model I can only be applied without large errors for small values of $[K_L a \tau_G]$. A simple approximation, $(K_L a)/(K_L a_{II}) = 1.0 + [K_L a \tau_G]$, is used to obtain approximate deviation values. This curve is also shown in Figure 1.

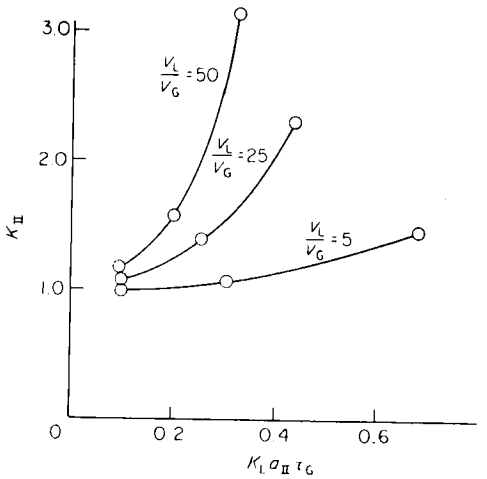

Figure 2. Factors to be used in correcting $K_L a$ values obtained from model II as a function of system parameters.

Data from Figure 1 can be replotted in a form which is easier to use. Thus in Figure 2 the correction factor, K_{II}, is plotted *vs* apparent values of $[K_L a \tau_G]$ or $[K_L a_{II} \tau_G]$, for various values of $[V_L/V_G]$. To correct $K_L a_{II}$ values, the gas mean residence time, $\tau_G = V_G/G$, must be known as well as $[V_L/V_G]$. The corrected value is obtained from the relation, $K_L a = K_{II} . K_L a_{II}$. From Figure 2 it is apparent that K_{II} is approximately unity when $[K_L a_{II} \tau_G] < 0.1$ for all values of $[V_L/V_G]$.

The use of Figure 2 to correct for gas dynamics is best shown by numerical example as follows. A fermenter of 100 litre liquid volume operates under aeration conditions with a volume of 110 litres. Thus, $[V_L/V_G] = 10$. The liquid is degassed with nitrogen; the gas stream is switched to air and the concentration of dissolved oxygen is measured with a very rapidly responding electrode.[6] Model II is assumed to be valid and the data is plotted logarithmically to obtain the slope $K_L a_{II}$. The value obtained is 0.083 s^{-1}. The aeration rate is 1 VVM or 100 litres/min. The mean gas residence time is thus 10/100 = 0.1 min or 6 s. $[K_L a_{II} \tau_G] = (0.083).(6.0) = 0.5$. Locating $[K_L a_{II} \tau_G] = 0.5$ on the graph and interpolating between the curves to locate $[V_L/V_G] = 10.0$ gives the approximate correction factor $K_{II} = 1.75$. Thus the true value of $K_L a = (1.75).(0.083) = 0.145\ s^{-1}$.

Recent workers[2] have applied the steady state oxygen balance, model IV, to their systems. It is of interest to investigate the errors resulting when assuming model IV to be valid for particular values of the governing parameters. Deviations in $K_L a$, $(K_L a - K_L a_{IV})/K_L a$, are plotted *vs* $[K_L a \tau_G]$ for various values of $[V_L/V_G]$ in Figure 3. From these curves, and comparing with Figure 1, it is clear that model IV does not

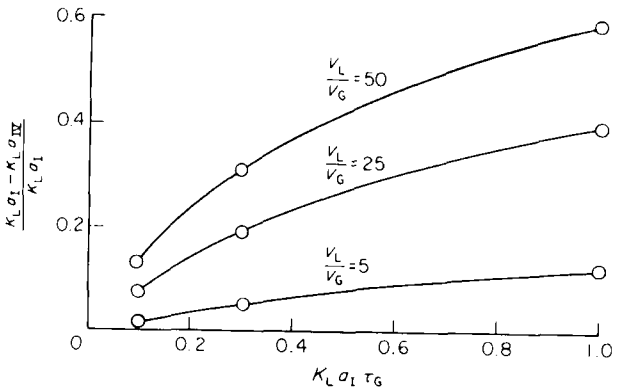

Figure 3. Fractional error in $K_L a$ accrued from model IV.

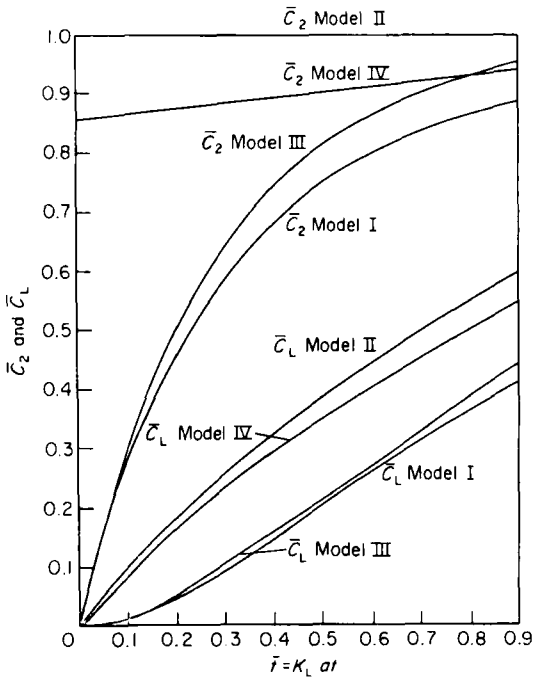

Figure 4. Computer simulations showing the dynamic response of the gas and liquid phases for models I, II, III and IV. $K_L a \tau_G = 0.3$; $V_L/V_G = 20.0$.

represent an appreciable improvement over model II. The errors for all parametric values are approximately the same.

That this is correct can be qualitatively concluded from comparison of the numerical solutions of models I, II, III and IV plotted in Figure 4 for parametric values $[K_L a \tau_G] = 0.3$ and $[V_L/V_G] = 20$. Here the dimensionless gas and liquid phase concentrations are plotted against dimensionless time. The steady state model IV does

not exhibit gas concentrations that are appreciably different from model II ($\bar{C}_2 = \bar{C}_{air} = 1.0$). Model III shows a response of the gas phase which follows the true situation, model I, more closely. The effect of the gas phase dynamics on the liquid phase oxygen concentration is shown for all three models. No extensive comparison of model III with alternative models has been undertaken here except to show, on the basis of Figure 4, that $K_L a_{III}$ values can generally be expected to lie closest to those of model I. It should be pointed out that model III, when used with the first order electrode dynamic equation, represents a system of equations (three first-order lag equations in series), which can be analytically integrated. The analytical solution can be most useful when obtaining $K_L a$ by parameter estimation computer methods. Model I possesses no such analytical solution.

Solutions of models I and II, together with the electrode model, provide data to calculate the apparent $K_L a$ value, $K_L a_{IIE}$. Thus, in Figure 5 the deviation$(K_L a - K_L a_{IIE})/$

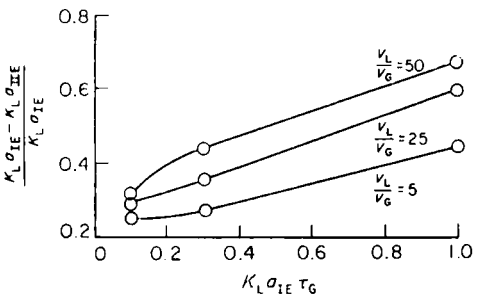

Figure 5. Fractional error arising from the combination of model II and the electrode response model. The electrode parameter, $K_L a_{IE} \tau_E$, is constant and equals 0.75.

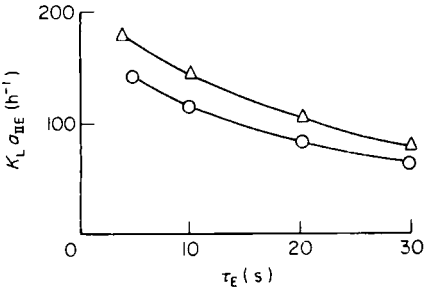

Figure 6. The effect of electrode response time on the apparent $K_L a$ value for typical fermenter conditions. △, Approximation; ○, simulation; VVM, = 1.0; $K_L a$, 0.083 s^{-1} = 300 h^{-1}; τ_E = 20.0 s; V_L/V_G = 20.0.

$K_L a$, is plotted *vs* $[K_L a \tau_G]$ for various values of $[V_L/V_G]$ and constant $[K_L a \tau_E] = 0.75$.

This graph demonstrates the importance of including the electrode dynamics for even rather rapidly responding devices. For example, a system exhibiting $K_L a = 300$ h^{-1} with an electrode response $\tau_E = 11$ s, would possess an electrode parameter $[K_L a \tau_E] = 0.9$. The deviations would be larger in this case than shown in Figure 5.

Exactly how electrode responses can produce $K_L a$ deviations in a specific fermentation system is shown in Figure 6. Here $K_L a_{IIE}$ is plotted *vs* τ_E for the following fermenter measurement conditions:

$$K_L a = 300 \text{ h}^{-1}, \text{ flow rate} = 1.0 \text{ VVM}, [V_L/V_G] = 20.0$$

The apparent $K_L a$ varies between 150 h^{-1} and 60 h^{-1} as τ_E ranges from 5 to 30 s. The approximately 100% error for very fast electrodes is caused by the gas dynamic effects inherent in using model II. An approximate curve is presented in Figure 6. This is obtained by setting the correction factor for both the gas and electrode dynamics, $K_{IIE} = 1.0 + [K_L a \tau_G] + [K_L a \tau_E]$, where $K_L a_{IIE} = K_L a / K_{IIE}$. This simple correction formula can be used to obtain the approximate correction factor.

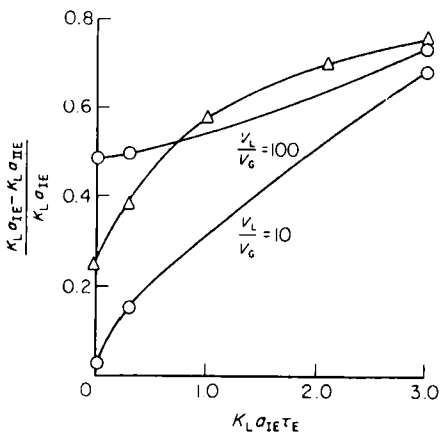

Figure 7. Fractional error in $K_L a$ arising from various electrode parameters. $K_L a_{IE} \tau_G$ is constant and equal to 0.3. ○, Simulation; △, approximation.

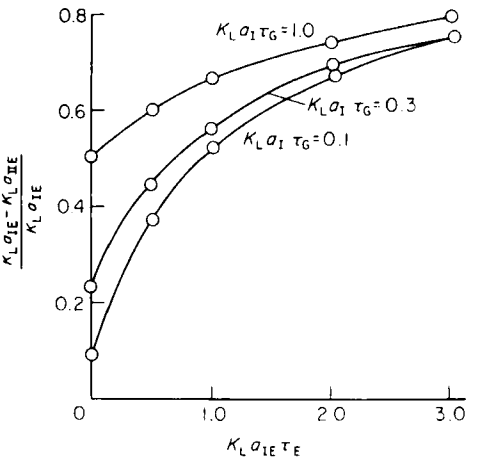

Figure 8. Approximate fractional $K_L a$ error as a function of $[K_L a \tau_G]$ and $[K_L a \tau_E]$, useful in correcting apparent $K_L a$ values for gas and electrode dynamic effects.

Presented more generally in Figure 7 the $K_L a$ deviation, $(K_L a - K_L a_{IIE})/K_L a_I$ is plotted *vs* $[K_L a \tau_E]$ for various $[V_L/V_G]$ and constant $[K_L a \tau_G] = 0.3$. The approximation $K_{IIE} = 1.0 + [K_L a \tau_G] + [K_L a \tau_E]$ is used to calculate the approximate deviation. As seen in Figure 7 the approximation is accurate for $[V_L/V_G] = 100$ and $[K_L a \tau_E] > 0.5$.

Using this approximate correction for various $[K_L a \tau_G]$ values, the deviations in $K_L a$ are plotted in Figure 8 against $[K_L a \tau_E]$. These curves are not based on exact simulations but are developed from the above approximation for K_{IIE}. They can be expected to be valid within 10–20% for $[V_L/V_G] = 100.0$.

A plot of apparent values of $[K_L a \tau_E]$ *vs* the correction factor K_{IIE} is particularly useful in correcting data from experiments. Figure 9 presents curves of K_{IIE} *vs* $[K_L a \tau_G]$ for various values of $[K_L a . \tau_G]$. Shown also on these curves are the numerical values of $K_L a_{IIE} \tau_G$. These curves are based on the approximation and are shown for comparison. The use of Figure 9 is similar to the use of Figure 2. Values of τ_G and τ_E must be estimated. The logarithmic plot of experimental data gives $K_L a_{IIE}$ as slope. This allows the calculation of $[K_L a_{IIE} \tau_G]$ and $[K_L a_{IIE} . \tau_E]$. When $[V_L/V_G] > 50.0$ and $0.25 < K_L a \tau_G < 1.0$, the approximations give estimates of the correction factor within 20%. When $[V_L/V_G] > 50.0$ an exact numerical solution should be undertaken.

4. Conclusions

The dynamic method for $K_L a$ determination is subject to large errors resulting from incorrect dynamic models. The nature of the dynamic experiment requires that careful consideration be given to the gas phase dynamics. Depending on the parameters of the system, neglecting the transient nature of the gas phase can lead to intolerable errors. Dynamic lags in the membrane oxygen electrode can be described by a simple

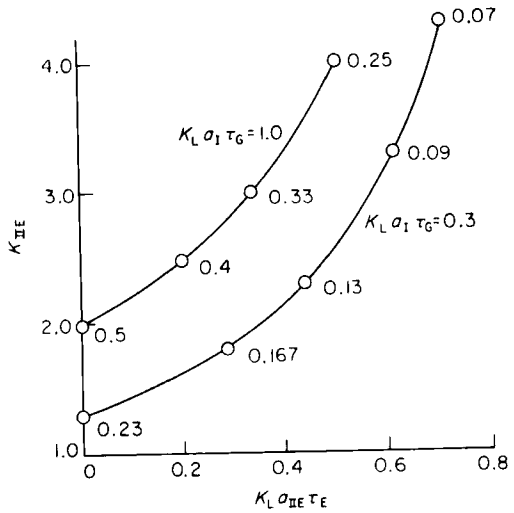

Figure 9. Correction factors plotted as a function of apparent parametric values, $[K_L a_{II\varepsilon} \tau_\varepsilon]$ and $[K_L a_{II\varepsilon} \tau_G]$. Numbers on lines denote $K_L a_{II\varepsilon} \tau_G$ values.

model which, when combined with the gas and liquid phase models, provides a means of estimating the desired $K_L a$ parameter.

Acknowledgements

One of the authors (A.E.) acknowledges the support of the Kommission zur Förderung Wissenschaftlicher Forschung, grant number 91.2. This work was accomplished under a cooperative programme in biochemical engineering under the direction of Professor J. R. Bourne and Professor A. Fiechter.

Appendix

Symbols

C	Oxygen concentration (mol/litre)
$\bar{C}$	Dimensionless concentration
C_L^*	Equilibrium concentration (mol/litre)
G	Gas flow rate (litre/unit time)
H	Henry's coefficient $= L^2/t^2$
K	Integration constant and correction factor for $K_L a$
$K_L a$	Oxygen mass transfer coefficient based on liquid volume and concentration driving force (t^{-1})
P	Partial pressure
R	Gas constant
T	Temperature, absolute
t	Time, t
$\bar{t}$	Dimensionless time

V_G Volume of dispersed gas in the liquid (litres)
V_L Volume of liquid in the fermenter (litres)
VVM Volumetric air flow per minute per fermenter volume (min^{-1})
Δ Refers to K_La differences
τ Mean residence time and electrode time constant (t)

Subscripts

E Refers to electrode and electrode dynamic model
L Refers to liquid phase
G Refers to gas phase
1, 2 Refers to inlet and outlet gas
i, j Refers to components i and j
I Refers to model I
II Refers to model II
III Refers to model III
IV Refers to model IV

References

1. Cooper, C. M.; Fernstrom, G. A.; Miller, S. A. *Ind. Engng Chem.* 1944, **36**, 504.
2. Robinson, C. W.; Wilke, C. R. *Biotechnol. Bioengng* 1973, **15**, 755.
3. Calderbank, P. H. *Trans. Instn Chem. Engrs* 1959, **37**, 173.
4. Bandyopadhyay, B.; Humphrey, A. E.; Taguchi, H. *Biotechnol. Bioengng* 1967, **9**, 533.
5. Aiba, S.; Huang, S. Y. *Chem. Engng Sci.* 1969, **24**, 1149.
6. Topiwala, H. H.; Hamer, G. *Trans. Instn Chem. Engrs* 1974, **52**, 113.
7. Heineken, F. G. *Biotechnol. Bioengng* 1970, **12**, 145.
8. Linek, V.; Sobotka, M.; Prokop, A. *Biotechnol. Bioengng* 1973, **15**, 429.
9. Hanhart, J.; Kramers, H.: Westerterp, K. R. *Chem. Engng Sci.* 1963, **18**, 503.